Science

REPORTS

Cite as: J. Major *et al.*, *Science* 10.1126/science.abc2061 (2020).

Type I and III interferons disrupt lung epithelial repair during recovery from viral infection

Jack Major[1], Stefania Crotta[1], Miriam Llorian[2], Teresa M. McCabe[1]*, Hans Henrik Gad[3], Simon L. Priestnall[4,5], Rune Hartmann[3], Andreas Wack[1]†

[1]Immunoregulation Laboratory, The Francis Crick Institute, London, UK. [2]Bioinformatics and Biostatistics, The Francis Crick Institute, London, UK. [3]Department of Molecular Biology and Genetics, Aarhus University, Aarhus, Denmark. [4]Department of Pathobiology & Population Sciences, The Royal Veterinary College, Hatfield, UK. [5]Experimental Histopathology STP, The Francis Crick Institute, London, UK.

*Present address: Adaptive Immunity Research Unit, Glaxosmithkline, Stevenage, UK.

†Corresponding author. Email: andreas.wack@crick.ac.uk

Excessive cytokine signaling frequently exacerbates lung tissue damage during respiratory viral infection. Type I (IFN-α/β) and III (IFN-λ) interferons are host-produced antiviral cytokines. Prolonged IFN-α/β responses can lead to harmful proinflammatory effects, whereas IFN-λ mainly signals in epithelia, inducing localized antiviral immunity. Here we show that IFN signaling interferes with lung repair during influenza recovery, with IFN-λ driving these effects most potently. IFN-induced p53 directly reduces epithelial proliferation and differentiation, increasing disease severity, and susceptibility to bacterial superinfections. Thus, excessive or prolonged IFN-production aggravates viral infection by impairing lung epithelial regeneration. Therefore, timing and duration are critical parameters of endogenous IFN action and should be considered carefully for IFN therapeutic strategies against viral infections like influenza and coronavirus disease 2019 (COVID-19).

During infection with respiratory viruses, disease severity is linked to lung epithelial destruction, due to both cytopathic viral effects and immune-mediated damage. Epithelial loss contributes to acute respiratory distress syndrome, pneumonia, and increased susceptibility to bacterial superinfections. Restoration of damaged epithelial tissues is therefore paramount in order to maintain lung function and barrier protection.

Interferons (IFNs) are key to the antiviral host defense. IFN-α/β and IFN-λ are induced upon viral recognition and trigger transcription of interferon-stimulated genes with antiviral function in infected and bystander cells. Due to widespread expression of the type I IFN receptor (IFNAR) in immune cells, IFN-α/β responses can result in immunopathology during viral infections, including influenza virus and severe acute respiratory syndrome coronavirus (SARS-CoV-1) (*1*–*4*). The IFN-λ receptor (IFNLR) is mainly expressed at epithelial barriers, and responses are therefore often characterized by their ability to confer localized antiviral protection at the site of infection, without driving damaging proinflammatory responses associated with IFN-α/β. In addition to antiviral and proinflammatory activity, IFNs exert antiproliferative and proapoptotic functions (*5*). Despite a growing understanding of immunopathology in respiratory viral infection, it is unknown how IFN responses affect lung epithelial repair.

Influenza virus infection in C57BL/6 (B6) wild-type (WT) mice resulted in weight loss, accompanied by significant immune cell infiltration and lung damage (fig. S1, A to D). Recovery from infection coincided with the onset of epithelial regeneration (fig. S1, C and D). To further investigate the dynamics of lung repair following influenza virus infection, epithelial cell proliferation was analyzed by flow cytometry, using the proliferation marker Ki67 (gating strategy in fig. S2). During steady-state conditions, type II alveolar epithelial cells (AT2; $EpCam^{+}MHCII^{+}CD49f^{lo}$) (*6*–*8*) showed a low rate of turnover (Fig. 1A). However, following influenza virus-induced lung damage, AT2 cells underwent rapid proliferation starting at days 5-7 post infection, correlating with mouse recovery and weight gain (Fig. 1A and fig. S1B).

To compare the dynamics of epithelial recovery with IFN production, we analyzed IFN subtypes (IFN-α, IFN-β, and IFN-λ) in bronchoalveolar lavage fluid (BALF) throughout infection. IFNs were produced rapidly, peaking 2 days post infection (Fig. 1B). The magnitude of IFN-λ production was significantly greater than that of IFN-α/β, both in duration and in length of peak production. Importantly, only IFN-λ was detected 7–8 days post infection, coinciding with the onset of epithelial recovery (Fig. 1, A and B). Thus, following influenza virus infection, signaling triggered by IFNs, in particular by IFN-λ, overlaps with the onset of lung repair.

To compare the effects of equipotent amounts of IFN-α, IFN-β, and IFN-λ on lung repair, mice were treated during recovery from influenza virus infection (7 to 10 days post

infection; figs. S3A and S4). To study the effects of IFN treatment specifically on epithelial cells, we generated irradiation bone marrow (BM) chimeras in which WT recipients were given *Ifnar1*$^{-/-}$ BM cells, thus restricting IFNAR expression to the stromal compartment.

In chimeric mice, both IFN-α and IFN-β treatments significantly reduced the proliferation of AT2 cells on day 11 post influenza virus infection (Fig. 1C). Similarly, IFN-λ treatment reduced AT2 cell proliferation in WT mice (Fig. 1D). Reductions in proliferation were independent from changes in viral burden (fig. S3, B and C). The IFN-λ-mediated reduction in AT2 cell proliferation did not require IFN-λ signaling in neutrophils (*9*–*11*), as neutrophil depletion in WT mice using an anti-Ly6G monoclonal antibody had no effect (fig. S3, D and E). A caveat when using inbred mouse strains for influenza virus infection is the lack of a functional Mx1 protein, a crucial IFN-inducible influenza virus restriction factor in both mice and humans (*12*). We therefore infected mice expressing functional Mx1 alleles (B6-Mx1) with the influenza virus strain hvPR8-ΔNS1 for a more clinically relevant influenza model. IFN-λ treatment significantly reduced epithelial proliferation in the presence of functional Mx1 as well (Fig. 1E).

We next used *Ifnar1*$^{-/-}$ and *Ifnlr1*$^{-/-}$ mice to determine the role of endogenous IFNs during lung repair. AT2 cells were analyzed on day 8 post influenza virus infection, the time when IFN signaling and epithelial cell proliferation overlapped (Fig. 1, A and B). Both *Ifnar1*$^{-/-}$ and *Ifnlr1*$^{-/-}$ mice had improved AT2 cell proliferation, compared to WT controls (Fig. 1, F and G). This was dependent on IFN signaling specifically through the epithelium, as receptor deficiency in the stromal compartment alone was sufficient to increase lung epithelial cell proliferation (Fig. 1H). Improved proliferation was independent of major changes in viral burden (fig. S5A). Viral control in individual IFN receptor-knockout mice was likely unaffected due to redundancy between type I and III IFN antiviral responses in epithelial cells (*13*, *14*). Despite type I and III IFN redundancy in viral control (fig. S5A), the lack of redundancy in antiproliferative IFN responses, with both *Ifnar1*$^{-/-}$ and *Ifnlr1*$^{-/-}$ mice displaying enhanced epithelial proliferation (Fig. 1, F to H), led us to further interrogate the phenotype. IFNAR signaling has previously been shown to be important for the production of IFN-λ during influenza virus infection (*15*, *16*). Consistently, we observed a significant reduction in IFN-λ (and indeed IFN-α/β) production in *Ifnar1*$^{-/-}$ mice compared to WT, yet we saw little change in IFN-α/β levels in *Ifnlr1*$^{-/-}$ mice (fig. S5B). Thus, the improved epithelial proliferation in *Ifnar1*$^{-/-}$ mice may result from reduced IFN-λ. IFN production defects in *Ifnar1*$^{-/-}$ mice are linked to reduced steady-state priming in the absence of tonic IFNAR activation in immune cells (*17*). To circumvent this, we administered an anti-IFNAR monoclonal antibody (MAR1-5A3) only from the onset of influenza virus infection. Anti-IFNAR treatment maintained steady-state priming required for IFN-λ production (fig. S5C), despite blocking IFN-α/β signaling through IFNAR (fig. S5D). Importantly, anti-IFNAR treatment from day 0 or day 3 post infection had no effect on lung epithelial cell proliferation (fig. S5E). Thus, in murine influenza virus infection, endogenous IFN-λ responses are most effective in disrupting epithelial regeneration during influenza recovery, through direct effects on epithelial cells.

To understand mechanistically how IFNs exert the observed antiproliferative effects, we set up primary murine airway epithelial cell (AEC) cultures. AECs undergo rapid proliferation and differentiation upon exposure to an air-liquid interface (ALI), recapitulating lung repair processes observed in vivo (*18*, *19*). IFNs used for in vitro assays were titrated on AEC cultures, to compare IFN subtypes at equivalent biological potency (fig. S6). All three IFN subtypes significantly impaired the growth of AEC cultures, with IFN-β and IFN-λ having the most significant effects (Fig. 2, A to C, and fig. S7A). Similar effects were observed when primary human AEC cultures were treated with equivalent doses of IFN subtypes (Fig. 2D). Growth inhibitory effects were dependent on the presence of the respective IFN receptor (fig. S7B). IFN-β or IFN-λ treatment increased the frequency of apoptotic or necrotic cells (Annexin V^{+}/TO-PRO-3^{+}) (fig. S7, C and D). However, the growth inhibitory effects of IFNs were only observed in actively dividing cultures (fig. S7, E to G). Thus, the increase in apoptosis observed may occur as a result of failed progression through the cell cycle following IFN treatment, as seen previously (*20*).

We next examined the effects of IFNs on AEC differentiation. Following acute damage, populations of basal cells and Scgb1a1^{+} secretory cells give rise to secretory and multiciliated cell subtypes (*21*). To study effects of IFNs on AEC differentiation, we initiated IFN treatment late during the course of AEC growth, during air exposure, when AEC differentiation is induced (fig. S8A). IFN-β and IFN-λ treatment significantly reduced the expression of genes pertaining to multiciliated (*Mcidas* and *Ccno*) and secretory cell (*Muc5AC* and *Scb1a1*) differentiation (Fig. 2F). Expression of the basal cell marker *Krt5* remained unchanged, or was increased by IFN-λ treatment, suggesting maintenance of stemness (fig. S8B). We also found reduced numbers of multiciliated cells in AEC cultures (acetylated α-tubulin^{+}) following IFN-λ treatment, but not with IFN-α or IFN-β (Fig. 2G and fig. S8C). In vivo, *Ifnlr1*$^{-/-}$ mice displayed increased multiciliated cells in repairing conducting airways on day 10 post influenza virus infection (Fig. 2H). Using flow cytometry, we quantified this increase in the frequency of differentiated AECs (EpCam^{hi}CD49f^{hi}CD24^{+}), composed of multiciliated, goblet, and club cells (Fig. 2I and fig. S2) (*22*). Thus, IFN-λ signaling reduces the capacity for basal cell differentiation during recovery from influenza virus infection.

To understand how IFNs mediate antiproliferative effects, we performed RNA-sequencing on IFN-treated AEC cultures (Fig. 3A). Principal component analysis (PCA) clustered 4-hour IFN treated samples together regardless of subtype (Fig. 3B), confirming equal subtype dosage based on previous titrations (fig. S9A). Five-days of IFN-β or IFN-λ treatment clustered AECs together separate from untreated controls on both PC1 and PC2 (Fig. 3B). Gene ontology analysis confirmed genes contributing to this variance are involved in IFN-signaling and epithelial cell development (supplementary text and fig. S9B). Ingenuity Pathway Analysis revealed induction of pathways regulating cell cycle and cell death following prolonged IFN treatment, most significantly induced by IFN-λ across all timepoints (Fig. 3C). Predicted upstream transcriptional regulators identified typical regulators of IFN function, including STAT and IRF proteins, in addition to cell cycle regulators (Fig. 3D). We identified the tumor suppressor protein p53 as a top candidate regulating IFN-inducible antiproliferative effects. p53 has previously been shown to directly regulate IFN-α/β antitumor responses (*23*). Gene set enrichment analysis (GSEA) identified IFN-mediated induction of the p53 pathway (fig. S9C), and we identified induction of p53-regulated downstream targets in expression data (fig. S9D). To confirm the role of p53, we utilized *Tp53*$^{-/-}$ AEC cultures. IFN-mediated reduction in AEC growth, differentiation, and induction of antiproliferative downstream p53 target genes *Gadd45 g* and *Dusp5* (*24*, *25*) was p53-dependent, with no changes observed in *Tp53*$^{-/-}$ AECs (Fig. 3, E to G, and fig. S9E). We next examined whether IFNs regulate p53 activity in epithelial cells during lung repair in vivo. To study IFN effects specifically in the lung epithelium, we once again generated *Ifnar1*$^{-/-}$ → WT BM chimeric mice for IFN-α or IFN-β treatment, or depleted neutrophils in WT mice with anti-Ly6G for IFN-λ treatment (fig. S3A). IFN-β and IFN-λ, but not IFN-α, significantly up-regulated p53 expression in repairing lung epithelial cells (Fig. 3, H and I). Thus, IFN-β and IFN-λ mediate antiproliferative effects in AECs via the induction of p53.

Our data supports a key role for IFN signaling, particularly IFN-λ, in the reduction of epithelial proliferation and differentiation during lung repair. We therefore tested whether IFNs alter the state or barrier function of lung epithelia. RNA-sequencing of sorted lung epithelial cells (EpCam^{+}CD31^{-}CD45^{-}) from influenza virus-infected WT or *Ifnlr1*$^{-/-}$ mice confirmed an up-regulation of pathways pertaining to proliferation and multiciliogenesis in *Ifnlr1*$^{-/-}$ mice (Fig. 4A). Improved repair correlated with reduced lung damage, with a reduction in both the total, and red blood cell number in the BALF of *Ifnlr1*$^{-/-}$ mice day 8 post infection (Fig. 4, B and C, and fig. S10A). Additionally, *Ifnlr1*$^{-/-}$ mice had fewer immune cells infiltrating lung tissue (Fig. 4D). In humans, influenza virus-induced epithelial damage increases susceptibility to infection by opportunistic bacterial pathogens, including *S. pneumoniae* (*26*). To measure the effects of IFN-λ on lung barrier function, we challenged influenza virus-infected mice with *S. pneumoniae*. Both full IFNLR knockout mice, and mice lacking IFNLR in the stromal compartment (WT → *Ifnlr1*$^{-/-}$), had improved survival following bacterial superinfection (Fig. 4E and fig. S10B). Thus, IFN-λ signaling reduces the capacity for epithelial repair, resulting in prolonged lung damage, compromised barrier function, and increased susceptibility to bacterial superinfection.

Here we describe a mechanism by which type I and III IFN signaling aggravates lung pathology during respiratory viral infection. Although all three IFN subtypes reduced lung proliferation following treatment during influenza recovery, only endogenous IFN-λ compromised repair. This is likely due to increased IFN-λ production during infection combined with greater induction of antiproliferative pathways, compared to IFN-α/β. A recent study has shown that IFN-λ produced by dendritic cells inhibits lung epithelial repair following viral recognition (*27*). Influenza virus-infected macaques revealed an elevated IFN signature late during infection bronchial tissue (*28*). Additionally, COVID-19 patients displayed strong induction of IFN and p53 signaling in collected BALF (*29*). Analysis of lung tissue and BALF from respiratory virus infected patients experiencing severe disease will provide insight into the mechanisms regulating disease pathogenesis. IFN-λ treatment early during influenza virus infection is protective in mice, offering antiviral protection without the proinflammatory responses associated with IFN-α/β (*30*, *31*). By studying specific effects in the respiratory epithelium, we identify a mechanism by which IFN exacerbates respiratory virus disease, independent of immunomodulation. Our data indicate the need for effective regulation of host IFN responses, and the importance of timing and duration when considering IFNs as therapeutic strategies to treat respiratory virus infections. Optimal protection would be achieved by strong induction of IFN-stimulated genes early during infection to curb viral replication, followed by timely down-regulation of IFN responses, enabling efficient lung epithelial repair.

REFERENCES AND NOTES

1. J. R. Teijaro, C. Ng, A. M. Lee, B. M. Sullivan, K. C. F. Sheehan, M. Welch, R. D. Schreiber, J. C. de la Torre, M. B. A. Oldstone, Persistent LCMV infection is controlled by blockade of type I interferon signaling. *Science* **340**, 207–211 (2013). doi:10.1126/science.1235214 Medline
2. S. Davidson, S. Crotta, T. M. McCabe, A. Wack, Pathogenic potential of interferon αβ in acute influenza infection. *Nat. Commun.* **5**, 3864 (2014). doi:10.1038/ncomms4864 Medline
3. R. Channappanavar, A. R. Fehr, R. Vijay, M. Mack, J. Zhao, D. K. Meyerholz, S. Perlman, Dysregulated type I interferon and inflammatory monocyte-macrophage responses cause lethal pneumonia in SARS-CoV-infected mice. *Cell Host Microbe* **19**, 181–193 (2016). doi:10.1016/j.chom.2016.01.007 Medline
4. E. B. Wilson, D. H. Yamada, H. Elsaesser, J. Herskovitz, J. Deng, G. Cheng, B. J.

Aronow, C. L. Karp, D. G. Brooks, Blockade of chronic type I interferon signaling to control persistent LCMV infection. *Science* **340**, 202–207 (2013). doi:10.1126/science.1235208 Medline
5. B. S. Parker, J. Rautela, P. J. Hertzog, Antitumour actions of interferons: Implications for cancer therapy. *Nat. Rev. Cancer* **16**, 131–144 (2016). doi:10.1038/nrc.2016.14 Medline
6. K. Hasegawa, A. Sato, K. Tanimura, K. Uemasu, Y. Hamakawa, Y. Fuseya, S. Sato, S. Muro, T. Hirai, Fraction of MHCII and EpCAM expression characterizes distal lung epithelial cells for alveolar type 2 cell isolation. *Respir. Res.* **18**, 150 (2017). doi:10.1186/s12931-017-0635-5 Medline
7. A. N. Nabhan, D. G. Brownfield, P. B. Harbury, M. A. Krasnow, T. J. Desai, Single-cell Wnt signaling niches maintain stemness of alveolar type 2 cells. *Science* **359**, 1118–1123 (2018). doi:10.1126/science.aam6603 Medline
8. W. J. Zacharias, D. B. Frank, J. A. Zepp, M. P. Morley, F. A. Alkhaleel, J. Kong, S. Zhou, E. Cantu, E. E. Morrisey, Regeneration of the lung alveolus by an evolutionarily conserved epithelial progenitor. *Nature* **555**, 251–255 (2018). doi:10.1038/nature25786 Medline
9. K. Blazek, H. L. Eames, M. Weiss, A. J. Byrne, D. Perocheau, J. E. Pease, S. Doyle, F. McCann, R. O. Williams, I. A. Udalova, IFN-λ resolves inflammation via suppression of neutrophil infiltration and IL-1β production. *J. Exp. Med.* **212**, 845–853 (2015). doi:10.1084/jem.20140995 Medline
10. A. Broggi, Y. Tan, F. Granucci, I. Zanoni, IFN-λ suppresses intestinal inflammation by non-translational regulation of neutrophil function. *Nat. Immunol.* **18**, 1084–1093 (2017). doi:10.1038/ni.3821 Medline
11. V. Espinosa, O. Dutta, C. McElrath, P. Du, Y.-J. Chang, B. Cicciarelli, A. Pitler, I. Whitehead, J. J. Obar, J. E. Durbin, S. V. Kotenko, A. Rivera1, Type III interferon is a critical regulator of innate antifungal immunity. *Sci. Immunol.* **2**, eaan5357 (2017). doi:10.1126/sciimmunol.aan5357 Medline
12. O. Haller, P. Staeheli, M. Schwemmle, G. Kochs, Mx GTPases: Dynamin-like antiviral machines of innate immunity. *Trends Microbiol.* **23**, 154–163 (2015). doi:10.1016/j.tim.2014.12.003 Medline
13. M. Mordstein, G. Kochs, L. Dumoutier, J.-C. Renauld, S. R. Paludan, K. Klucher, P. Staeheli, Interferon-λ contributes to innate immunity of mice against influenza A virus but not against hepatotropic viruses. *PLOS Pathog.* **4**, e1000151 (2008). doi:10.1371/journal.ppat.1000151 Medline
14. S. Crotta, S. Davidson, T. Mahlakoiv, C. J. Desmet, M. R. Buckwalter, M. L. Albert, P. Staeheli, A. Wack, Type I and type III interferons drive redundant amplification loops to induce a transcriptional signature in influenza-infected airway epithelia. *PLOS Pathog.* **9**, e1003773 (2013). doi:10.1371/journal.ppat.1003773 Medline
15. P. Österlund, V. Veckman, J. Sirén, K. M. Klucher, J. Hiscott, S. Matikainen, I. Julkunen, Gene expression and antiviral activity of alpha/beta interferons and interleukin-29 in virus-infected human myeloid dendritic cells. *J. Virol.* **79**, 9608–9617 (2005). doi:10.1128/JVI.79.15.9608-9617.2005 Medline
16. N. A. Jewell, T. Cline, S. E. Mertz, S. V. Smirnov, E. Flaño, C. Schindler, J. L. Grieves, R. K. Durbin, S. V. Kotenko, J. E. Durbin, Lambda interferon is the predominant interferon induced by influenza A virus infection in vivo. *J. Virol.* **84**, 11515–11522 (2010). doi:10.1128/JVI.01703-09 Medline
17. D. J. Gough, N. L. Messina, C. J. P. Clarke, R. W. Johnstone, D. E. Levy, Constitutive type I interferon modulates homeostatic balance through tonic signaling. *Immunity* **36**, 166–174 (2012). doi:10.1016/j.immuni.2012.01.011 Medline
18. Y. You, E. J. Richer, T. Huang, S. L. Brody, Growth and differentiation of mouse tracheal epithelial cells: Selection of a proliferative population. *Am. J. Physiol. Lung Cell. Mol. Physiol.* **283**, L1315–L1321 (2002). doi:10.1152/ajplung.00169.2002 Medline
19. J. A. Zepp, E. E. Morrisey, Cellular crosstalk in the development and regeneration of the respiratory system. *Nat. Rev. Mol. Cell Biol.* **20**, 551–566 (2019). doi:10.1038/s41580-019-0141-3 Medline
20. P. S. Subramaniam, P. E. Cruz, A. C. Hobeika, H. M. Johnson, Type I interferon induction of the Cdk-inhibitor p21WAF1 is accompanied by ordered G1 arrest, differentiation and apoptosis of the Daudi B-cell line. *Oncogene* **16**, 1885–1890 (1998). doi:10.1038/sj.onc.1201712 Medline
21. B. L. M. Hogan, C. E. Barkauskas, H. A. Chapman, J. A. Epstein, R. Jain, C. C. W. Hsia, L. Niklason, E. Calle, A. Le, S. H. Randell, J. Rock, M. Snitow, M. Krummel, B. R. Stripp, T. Vu, E. S. White, J. A. Whitsett, E. E. Morrisey, Repair and regeneration of the respiratory system: Complexity, plasticity, and mechanisms of lung stem cell function. *Cell Stem Cell* **15**, 123–138 (2014). doi:10.1016/j.stem.2014.07.012 Medline
22. J. Quantius, C. Schmoldt, A. I. Vazquez-Armendariz, C. Becker, E. El Agha, J. Wilhelm, R. E. Morty, I. Vadász, K. Mayer, S. Gattenloehner, L. Fink, M. Matrosovich, X. Li, W. Seeger, J. Lohmeyer, S. Bellusci, S. Herold, Influenza virus infects epithelial stem/progenitor cells of the distal lung: Impact on Fgfr2b-driven epithelial repair. *PLOS Pathog.* **12**, e1005544 (2016). doi:10.1371/journal.ppat.1005544 Medline
23. A. Takaoka, S. Hayakawa, H. Yanai, D. Stoiber, H. Negishi, H. Kikuchi, S. Sasaki, K. Imai, T. Shibue, K. Honda, T. Taniguchi, Integration of interferon-α/β signalling to p53 responses in tumour suppression and antiviral defence. *Nature* **424**, 516–523 (2003). doi:10.1038/nature01850 Medline
24. M. L. Smith, I. T. Chen, Q. Zhan, I. Bae, C. Y. Chen, T. M. Gilmer, M. B. Kastan, P. M. O'Connor, A. J. Fornace Jr., Interaction of the p53-regulated protein Gadd45 with proliferating cell nuclear antigen. *Science* **266**, 1376–1380 (1994). doi:10.1126/science.7973727 Medline
25. K. Ueda, H. Arakawa, Y. Nakamura, Dual-specificity phosphatase 5 (DUSP5) as a direct transcriptional target of tumor suppressor p53. *Oncogene* **22**, 5586–5591 (2003). doi:10.1038/sj.onc.1206845 Medline
26. J. A. McCullers, The co-pathogenesis of influenza viruses with bacteria in the lung. *Nat. Rev. Microbiol.* **12**, 252–262 (2014). doi:10.1038/nrmicro3231 Medline
27. A. Broggi, S. Ghosh, B. Sposito, R. Spreafico, F. Balzarini, A. Lo Cascio, N. Clementi, M. De Santis, N. Mancini, F. Granucci, I. Zanoni, Type III interferons disrupt the lung epithelial barrier upon viral recognition, *Science* 10.1126/science.abc3545 (2020).
28. D. Kobasa, S. M. Jones, K. Shinya, J. C. Kash, J. Copps, H. Ebihara, Y. Hatta, J. H. Kim, P. Halfmann, M. Hatta, F. Feldmann, J. B. Alimonti, L. Fernando, Y. Li, M. G. Katze, H. Feldmann, Y. Kawaoka, Aberrant innate immune response in lethal infection of macaques with the 1918 influenza virus. *Nature* **445**, 319–323 (2007). doi:10.1038/nature05495 Medline
29. Z. Zhou, L. Ren, L. Zhang, J. Zhong, Y. Xiao, Z. Jia, L. Guo, J. Yang, C. Wang, S. Jiang, D. Yang, G. Zhang, H. Li, F. Chen, Y. Xu, M. Chen, Z. Gao, J. Yang, J. Dong, B. Liu, X. Zhang, W. Wang, K. He, Q. Jin, M. Li, J. Wang, Heightened innate immune responses in the respiratory tract of COVID-19 patients. *Cell Host Microbe* 10.1016/j.chom.2020.04.017 (2020). doi:10.1016/j.chom.2020.04.017 Medline
30. S. Davidson, T. M. McCabe, S. Crotta, H. H. Gad, E. M. Hessel, S. Beinke, R. Hartmann, A. Wack, IFNλ is a potent anti-influenza therapeutic without the inflammatory side effects of IFNα treatment. *EMBO Mol. Med.* **8**, 1099–1112 (2016). doi:10.15252/emmm.201606413 Medline
31. I. E. Galani, V. Triantafyllia, E.-E. Eleminiadou, O. Koltsida, A. Stavropoulos, M. Manioudaki, D. Thanos, S. E. Doyle, S. V. Kotenko, K. Thanopoulou, E. Andreakos, Interferon-λ mediates non-redundant front-line antiviral protection against influenza virus infection without compromising host fitness. *Immunity* **46**, 875–890.e6 (2017). doi:10.1016/j.immuni.2017.04.025 Medline
32. P. Staeheli, P. Dreiding, O. Haller, J. Lindenmann, Polyclonal and monoclonal antibodies to the interferon-inducible protein Mx of influenza virus-resistant mice. *J. Biol. Chem.* **260**, 1821–1825 (1985). Medline
33. G. Kochs, L. Martínez-Sobrido, S. Lienenklaus, S. Weiss, A. García-Sastre, P. Staeheli, Strong interferon-inducing capacity of a highly virulent variant of influenza A virus strain PR8 with deletions in the NS1 gene. *J. Gen. Virol.* **90**, 2990–2994 (2009). doi:10.1099/vir.0.015727-0 Medline
34. C. Dellgren, H. H. Gad, O. J. Hamming, J. Melchjorsen, R. Hartmann, Human interferon-λ3 is a potent member of the type III interferon family. *Genes Immun.* **10**, 125–131 (2009). doi:10.1038/gene.2008.87 Medline
35. A. Horani, A. Nath, M. G. Wasserman, T. Huang, S. L. Brody, Rho-associated protein kinase inhibition enhances airway epithelial Basal-cell proliferation and lentivirus transduction. *Am. J. Respir. Cell Mol. Biol.* **49**, 341–347 (2013). doi:10.1165/rcmb.2013-0046TE Medline
36. C. L. Ward, M. H. Dempsey, C. J. Ring, R. E. Kempson, L. Zhang, D. Gor, B. W. Snowden, M. Tisdale, Design and performance testing of quantitative real time PCR assays for influenza A and B viral load measurement. *J. Clin. Virol.* **29**, 179–188 (2004). doi:10.1016/S1386-6532(03)00122-7 Medline
37. V. François-Newton, G. Magno de Freitas Almeida, B. Payelle-Brogard, D. Monneron, L. Pichard-Garcia, J. Piehler, S. Pellegrini, G. Uzé, USP18-based negative feedback control is induced by type I and type III interferons and

specifically inactivates interferon α response. *PLOS ONE* **6**, e22200 (2011). doi:10.1371/journal.pone.0022200 Medline
38. G. Schreiber, The molecular basis for differential type I interferon signaling. *J. Biol. Chem.* **292**, 7285–7294 (2017). doi:10.1074/jbc.R116.774562 Medline

ACKNOWLEDGMENTS

We are grateful to A. Suarez-Bonnet for histopathology scoring of lung H&E sections and to A. O'Garra, G. Stockinger, P. Staeheli, and D. Schnepf for critically reading the manuscript. We would like to thank Tinashe Matambanadzo for assistance performing animal procedures. We thank the Crick sequencing, histopathology, flow cytometry, and animal facilities for their excellent support. **Funding:** J.M., S.C., M.L., T.McC., S.L.P. and A.W. were supported by the Francis Crick Institute which receives its core funding from Cancer Research UK (FC001206), the UK Medical Research Council (FC001206), and the Wellcome Trust (FC001206). R.H. and H.H.G. were supported by Independent Research Fund Denmark | Medical Sciences, Research grant agreement 11-107588; and by Novo Nordisk Foundation, Grant agreement NNF190C0058287. **Author contributions:** Conception: A.W., S.C., and J.M; research design and experimentation: J.M., S.C., and T.McC.; data analysis: J.M., S.C., S.L.P. and M.L.; production and provision of key reagents: H.H.G. and R.H.; writing and editing of the manuscript: J.M., A.W., and S.C. All authors read and approved the final manuscript. **Competing interests:** The authors declare no competing interests. **Data and materials availability:** Gene expression data are deposited and available under the GEO accession code GSE148712. All other data supporting the findings of this study are available within the paper or in the supplementary materials.

SUPPLEMENTARY MATERIALS

science.sciencemag.org/cgi/content/full/science.abc2061/DC1
Materials and Methods
Supplementary Text
Figs. S1 to S10
Table S1
References (*32*–*38*)
MDAR Reproducibility Checklist
Data S1 to S3

21 April 2020; accepted 8 June 2020
Published online 11 June 2020
10.1126/science.abc2061

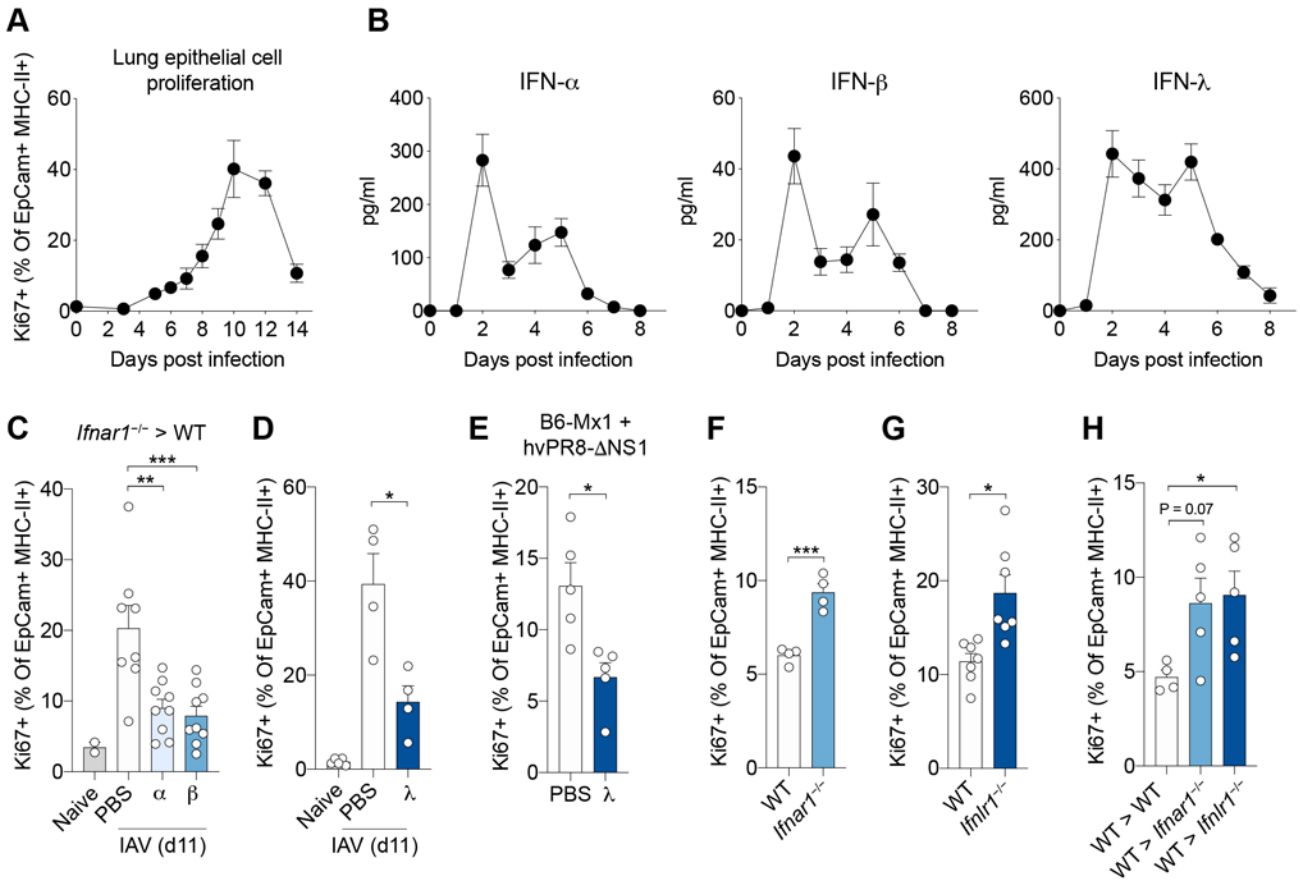

Fig. 1. Type I and III IFNs reduce epithelial cell proliferation during lung repair. (**A** and **B**) Mice were infected with 10^4 $TCID_{50}$ X31 (H3N2) influenza virus in 30 µl intranasally. (A) Proliferating ($Ki67^+$) AT2 cells ($EpCam^+MHCII^+CD49f^{lo}$) were measured by flow cytometry (n=5), and (B) type I and III IFN levels were detected in BALF (n=4) on indicated days post infection. (**C** and **D**) X31-infected mice were administered IFNs every 24 hours (on days 7 to 10 post infection). Proliferating ($Ki67^+$) AT2 cells ($EpCam^+MHCII^+CD49f^{lo}$) were measured by flow cytometry on day 11 post infection. (C) Lethally irradiated WT mice were injected with *Ifnar1*$^{-/-}$ bone marrow cells. Following reconstitution, influenza virus-infected chimeric mice were treated with PBS control (n=8), IFN-α (n=9), or IFN-β (n=9). Naïve controls are uninfected, untreated bone marrow chimeric mice (n=2). (D) Infected WT mice were treated with IFN-λ (n = 4) or PBS control (n = 4). Naïve controls are uninfected, untreated WT mice (n = 5). (**E**) B6-Mx1 mice were infected with 2.5×10^3 $TCID_{50}$ hvPR8-ΔNS1 (H1N1) and treated with IFN-λ (n = 4) or PBS control (n = 4) (IFN treatment and lung analysis was performed as for C and D). (**F** to **H**) Lungs from X31 infected WT (n=4 to 7), (F) *Ifnar1*$^{-/-}$ (n=4), (G) *Ifnlr1*$^{-/-}$ (n=7), and (H) BM chimeric mice (n=4 to 5) mice were harvested, and proliferating ($Ki67^+$) AT2 cells were measured by flow cytometry on day 8 post infection. All data are representative of at least two independent experiments. Data are shown as mean ± SEM and statistical significance was assessed by one-way ANOVA with Dunnett's post-test (C, D and H), or unpaired two-tailed Student's *t* test (E to G). ns, not significant (P>0.05); *P≤0.05, **P≤0.01, ***P≤0.001.

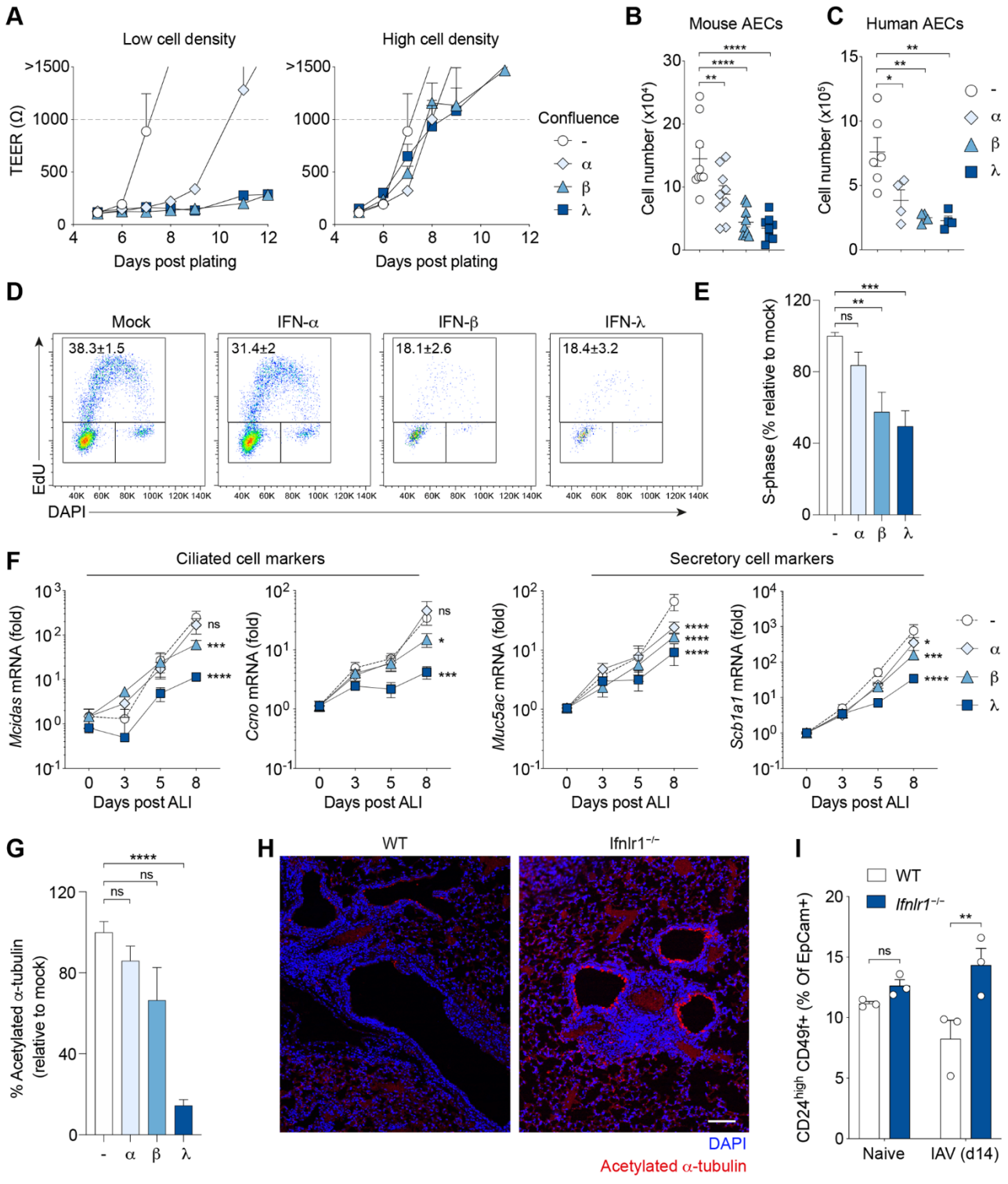

Fig. 2. IFN signaling blocks airway epithelial cell growth and differentiation. (**A**) Murine AECs were seeded at a low density (500 cells/transwell) or high density (10^4 cells/transwell) in the presence of equivalent doses of IFN-α, IFN-β, IFN-λ, or media control, and grown for 12 days (n=3 for all conditions). Confluence was determined by measuring transepithelial electrical resistance (TEER; >1000 Ω=confluent cultures). (**B**, **D**, and **E**) Proliferating murine AEC cultures (2 days prior to exposure to an ALI) were treated for 5 days with IFNs (day −2 pre ALI to day 3 post ALI), and effects on growth were determined by cell number (B) (n=9) and incorporation of the thymidine analog EdU to measure proliferation (D and E) (n=9). (**C**) Primary human AEC cultures were treated with IFNs for 5 days and cells were counted (n=4 to 6). (**F** and **G**) Murine AECs were grown to confluence, then exposed to an air–liquid interface (ALI) for 2 days. IFNs were then administrated for 6 days during ALI exposure (n = 6 for all conditions). Differentiation was determined by mRNA expression of the indicated genes (F) and the level of acetylated α-tubulin staining in cultures (G). (**H** and **I**) WT and *Ifnlr1*$^{-/-}$ mice were infected with influenza virus, and lungs were analyzed by immunofluorescence (DAPI/acetylated α-tubulin) on day 10 post infection (n=4) (H), and flow cytometry ($EpCam^+CD49f^{hi}CD24^+$) on day 14 post infection (n=3) (I). All data are representative of at least three independent experiments. Data are shown as mean ± SEM and statistical significance was assessed by one-way (B, C, E and G) or two-way (F and I) ANOVA with Dunnett's post-test. Scale bar represents 100 μm (H). ns, not significant (P>0.05); *P≤0.05, **P≤0.01, ***P≤0.001, ****P≤0.0001.

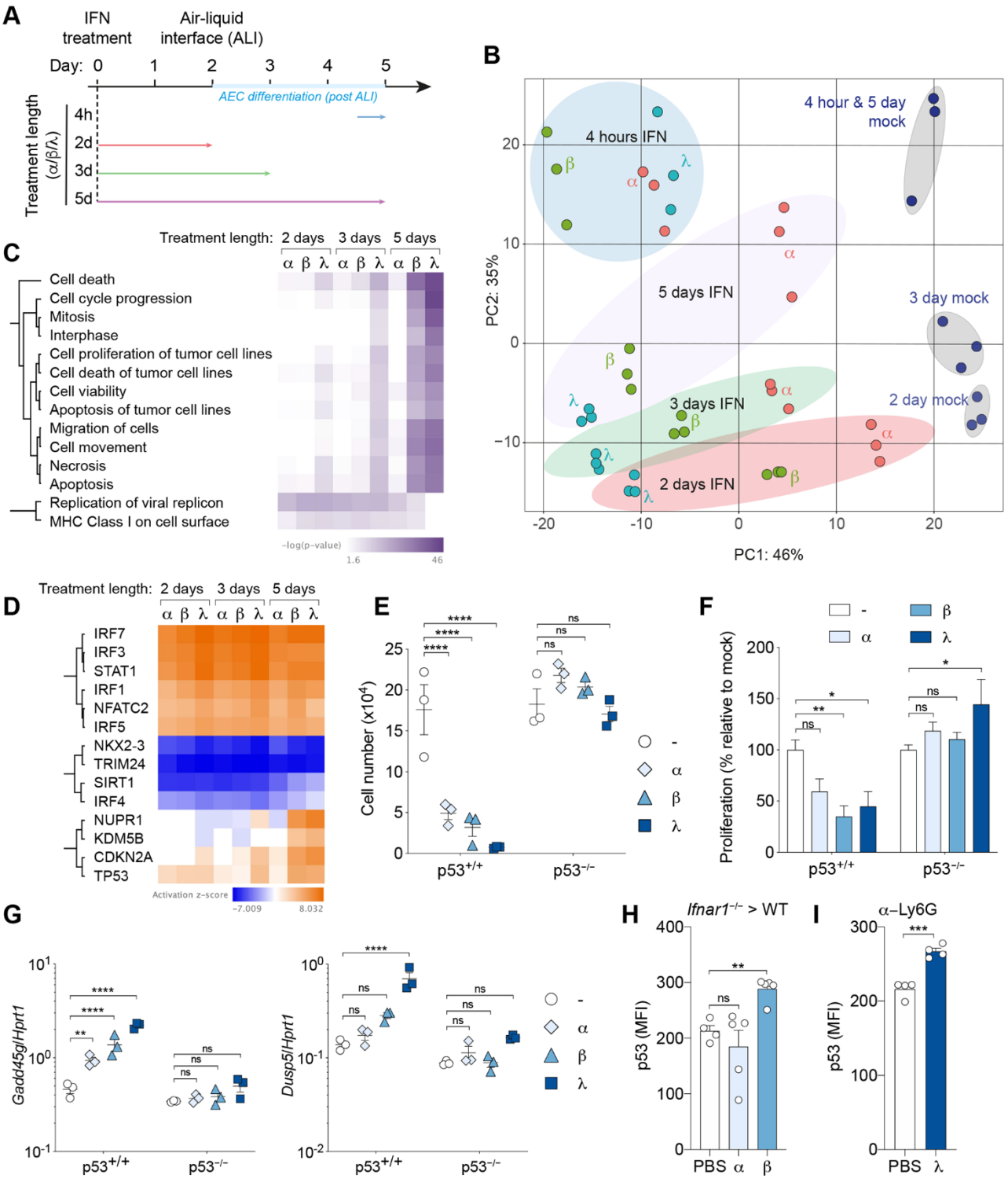

Fig. 3. Type I and III IFNs activate antiproliferative and cell death pathways in AECs via induction of p53. (**A**) Schematic diagram for IFN treatment of murine AECs for RNA-sequencing analysis. (**B**) PCA plot of RNA-sequencing data from AECs following IFN treatment, and untreated controls. (**C**) Heatmap for significant differences in "Canonical Pathways" for nine pairwise comparisons between indicated IFN treatment and the respective mock, at each time point (fold change >1.5, one-way ANOVA with Benjamini–Hochberg correction, $P<0.05$), Gene expression was compared using Ingenuity Pathway Comparison Analysis. (**D**) Predicted upstream transcriptional regulators of differentially expressed genes (Ingenuity Pathway Analysis). (**E** to **G**) WT and *p53*$^{-/-}$ murine AECs were treated with IFN subtypes for 5 days, and measured for growth by cell number (E), CFSE dilution (F), and mRNA expression of indicated genes (G) (n=3 for all conditions). (**H** and **I**) *Ifnar1*$^{-/-}$ → WT BM chimeric mice (H) (n=4 to 5) and α-Ly6G treated mice (I) (n=4) infected with influenza virus (X31), and treated with IFN every 24 hours consecutively for 4 days (days 7 to 10 post infection), before EpCam^{+}MHCII^{+}CD49f^{lo} AT2 cells were analyzed for p53 mean fluorescence intensity (MFI) on day 11 post infection by flow cytometry. All data are representative of at least two independent experiments (E to I). Data are shown as mean ± SEM and statistical significance was assessed by two-way (E to G) or one-way (H) ANOVA with Dunnett's post-test, or unpaired two-tailed Student's *t* test (I). ns, not significant ($P>0.05$); *$P\leq0.05$, **$P\leq0.01$, ***$P\leq0.001$, ****$P\leq0.0001$.

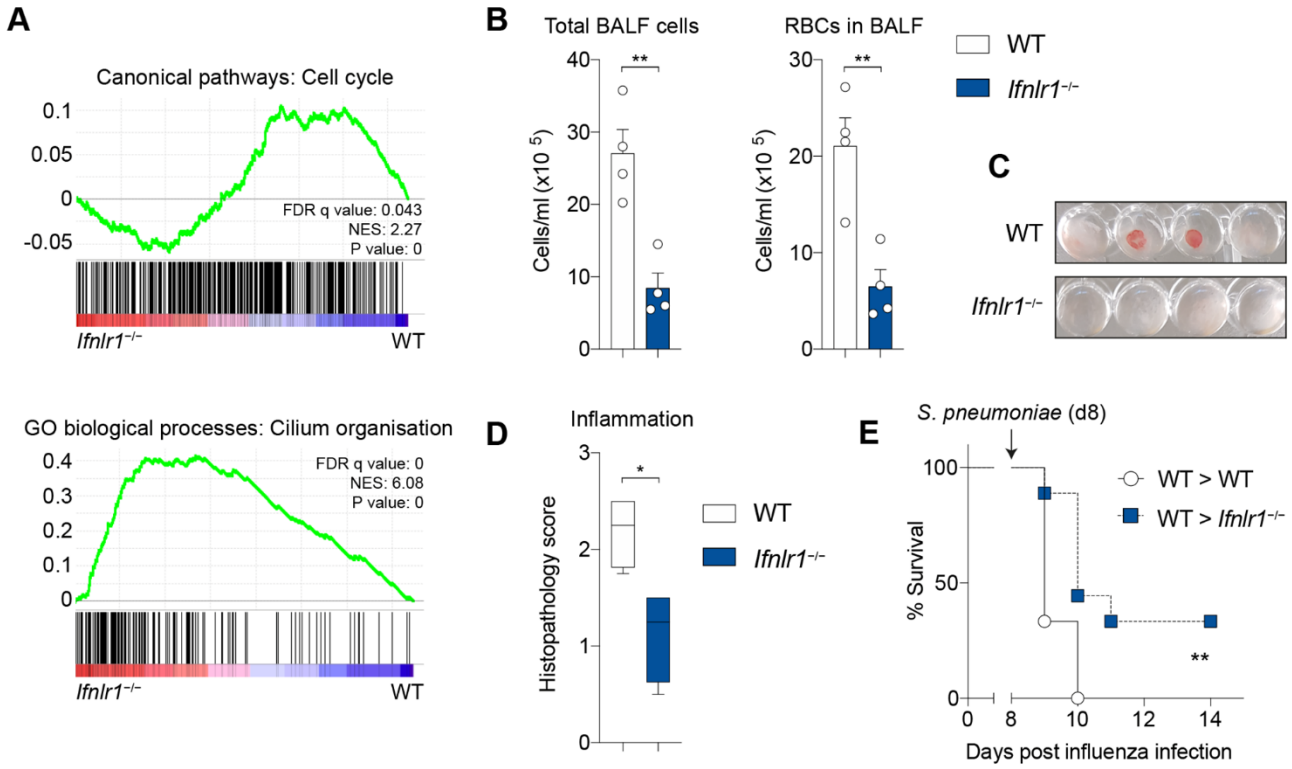

Fig. 4. *Ifnlr1*$^{-/-}$ mice have improved lung repair, reduced damage, and improved epithelial barrier function. WT and *Ifnlr1*$^{-/-}$ mice were infected with 10^4 $TCID_{50}$ X31 influenza virus (X31). (**A**) GSEA plots of RNA-sequencing datasets from WT or *Ifnlr1*$^{-/-}$ bulk lung epithelial cells (EpCam$^+$) on day 8 post infection. (**B** and **C**) Total cell and red blood cell (TER-119$^+$) number in BALF on day 8 post infection (n=4 for both WT and *Ifnlr1*$^{-/-}$ mice). (**D**) Histopathological analysis of H&E lung sections on day 9 post infection (n=4 for both WT and *Ifnlr1*$^{-/-}$ mice). (**E**) Lethally irradiated WT and *Ifnlr1*$^{-/-}$ mice were injected with WT bone marrow cells. Following reconstitution, chimeric mice were challenged with 2×10^5 colony-forming units (c.f.u.) TIGR4 in 30 µl on day 8 post influenza virus infection (n=8 WT, n=9 *Ifnlr1*$^{-/-}$). All data are representative of at least two independent experiments (B to E). Data are shown as mean ± SEM and statistical significance was assessed by unpaired two-tailed Student's *t* test (B), Mann–Whitney *U* test (D), or log-rank (Mantel–Cox) test (E, survival). *$P\leq0.05$, **$P\leq0.01$.

Type I and III interferons disrupt lung epithelial repair during recovery from viral infection

Jack Major, Stefania Crotta, Miriam Llorian, Teresa M. McCabe, Hans Henrik Gad, Simon L. Priestnall, Rune Hartmann and Andreas Wack

published online June 11, 2020

Science (print ISSN 0036-8075; online ISSN 1095-9203) is published by the American Association for the Advancement of Science, 1200 New York Avenue NW, Washington, DC 20005. The title *Science* is a registered trademark of AAAS.